DETECTION OF GOERTLER VORTICES IN HYPERSONIC FLOW

L. de Luca, G. Cardone and G.M. Carlomagno
University of Naples - DETEC
80125 Naples - ITALY

Abstract

The Goertler instability of hypersonic boundary layer flow and its influence on the wall heat transfer are experimentally analysed. Measurements, made in a wind tunnel by means of a computerized infrared (IR) imaging system, refer to the flow over 2D concave walls as well as 2D and 3D wedge models in viscous interaction regime. Wall temperature maps (that are to be interpreted as surface flow visualizations) and heat transfer spanwise fluctuations are presented. Measured vortices wavelengths are correlated to non-dimensional parameters and compared with numerical predictions of literature.

I. Introduction

Instability of a fluid flow can occur in a homogeneous medium owing to the streamlines curvature, e.g. in the boundary layer developing over a concave wall. The boundary layer centrifugal instability on a concave wall manifests itself in the form of counter-rotating streamwise vortices which are commonly referred to as Goertler vortices.

The study of the Goertler instability is of practical interest since the combined effects of the Tollmien-Schlichting waves and of the centrifugal force may drive the transition process in the boundary layer[1]. The presence of the vortices generally contributes to rise (both in compressible and incompressible regimes) the wall average heat transfer coefficient, even though very few quantitative measurements are available so far in the literature[2]. As regards the formation of Goertler vortices over the space shuttles surface during re-entry, in particular, owing to the relatively low thermal diffusivity of the materials used in the space technology, the vortices can produce a significant increase of the local heating that in turn imposes severe constraints to the thermal protection system.

Since the original Goertler work, such vortices have been matter of many theoretical and experimental works. Various authors have employed the linear instability theory to analyse the incompressible boundary layer behaviour along a concave wall; Floryan and Saric[3], for example, report a wide critical review. From the experimental point of view, the influence of the longitudinal curvature of a surface on the boundary layer stability was first analysed in the pioneering work of Liepmann[4]. Detailed experimental investigations are due to Bippes[5], which used the hydrogen-bubble technique to visualize the vortices, and Winoto and Low[1], which carried out velocity measurements by using a hot-wise anemometer and detected flow transition by means of a frequency spectrum method.

The works concerned with Goertler instability in compressible flow are later. Ginoux[6] observed the presence of Goertler vortices in the reattaching flow downstream of a descendent step at Mach number of 5.3. More recently El Hady and Verma[7], Spall and Malik[8], Jallade[9], Aymer de la Chevalerie et al.[10] published numerical papers about the compressible Goertler problem, including the pressure gradient as well as wall temperature influence. All these papers are concerned with the instability of supersonic and/or hypersonic flows over concave walls, having a constant streamwise curvature radius.

On the other hand, the experimental evidence shows that the boundary layer becomes unstable, leading to Goertler vortices, also in presence of a boundary layer-shock wave interaction due to a wedge (ramp or flap): e.g. Delery and Coet[11], Simeonides and Wendt[12], Alziary de Roquefort[13], de Luca and Cardone[14]. An analytical relationship for the flow curvature above the separation streamline is proposed in Ref.[15].

In the recent past, within the *Hermes* space project, University of

Naples and CEAT of Poitiers carried out a joint experimental investigation to measure the aerodynamic heating and to analyse the related flow field over a delta wing/flap configuration in order to study a 3D transitional shock/boundary layer interaction in hypersonic flow[16]. Attention was paid, in particular, on visualizing the presence of a spanwise periodic variation of the wall heat transfer coefficient over the flap, that is to be ascribed to the formation of Goertler vortices in the reattaching flow region. To the aim of obtaining a more basic knowledge about the formation of such vortices and of comparing experimental data with theoretical results, a particular study has been also carried out on special models, consisting of concave walls (producing a weak interaction regime) having a constant curvature radius.

This paper describes the experimental procedure and discuss the relevant data referring to the study about the presence of Goertler vortices on both the concave wall and wedge models tested in hypersonic flow, as well as their effect on the wall heat transfer. Present heat transfer measurements and surface flow visualizations has been performed by means of a computerized infrared (IR) imaging system.

II. Experimental set-up and data reduction

Experimental tests have been carried out in the hypersonic blowdown tunnel H210 of CEAT, Poitiers, having a test section diameter of 210 mm. The operating fluid is dry air which has typically a stagnation temperature $T_o = 800°K$ and a stagnation pressure $4.5\ MPa < p_o < 10 MPa$. Unit free stream Reynolds number Re_m is changed mainly by varying the stagnation pressure and, in present tests, ranges from $.89 \times 10^7/m$ to $2.1 \times 10^7/m$. Two nozzles have been employed to obtain nominal free stream Mach numbers equal to *7* and *8.15*, respectively. In effect, Mach number slightly depends on the stagnation pressure (due to the interaction of the nozzle boundary layer thickness) and ranges from *6.9* to *7.1* in the first case and from *8.0* to *8.2* in the other one[17].

At the beginning of each test run the model (which is initially in a remote position at room temperature) is vertically injected into the stream and subsequent time rise of its surface temperature is measured by viewing the model with an IR camera. A time sequence of thermograms (average time step is *0.24s*) is generally recorded during the test runs. Injection time is about *0.15s* and testing duration of a few seconds.

It has been shown[18] that at high Mach numbers, because of the high kinetic energy content of the stream, the detection of the model surface temperature by IR thermography can be performed by using it in the so-called *passive mode*. In fact, the strong aerodynamic heating makes possible the use of the IR camera without artificially creating a temperature difference between the model surface and the flow. In the present problem the spanwise periodic variation of the convective heat transfer coefficient produces a variation of the model surface temperature which allows the vortices detection by means of the IR technique. Thermograms may also be used to visualize the surface flow.

The concave wall models consist of two parts: a 2D flat plate which is followed by a concave wall, having a constant curvature radius (Fig. 1). Both the flat plate and the curved wall are made of melted NORCOAT 4000, a low thermal diffusivity material ($\alpha = 1.61 \times 10^{-7} m^2/s$), which is jointed to a stainless steel leading edge. The asperity produced by the junction, depending on the quality of the melting process, is of the order of a few tenth of millimeters. Three models have been tested. Denoting with L_1 the length of the flat plate, L_2 that of the curved part and $\Re$ the curvature radius, they are characterized respectively by:

a)	$L_1 = 0.05\ m$	$L_2 = 0.15\ m$	$\Re = 2\ m$
b)	$L_1 = 0.05\ m$	$L_2 = 0.12\ m$	$\Re = 1\ m$
c)	$L_1 = 0.10\ m$	$L_2 = 0.10\ m$	$\Re = 1\ m$

The NORCOAT material (which is made of silicon hollow microspheres drowned in a silicon elastomer base mixture) has been chosen because, owing to its relatively low thermal diffusivity coefficient, the thermal penetration depth is very small and the thin film sensor can be used to correlate wall temperature to heat transfer coefficient. Moreover, the thermal sensivity in detecting local temperature differences is enhanced. NORCOAT surface emissivity coefficient is sufficiently high (the measured value in the wavelength range of interest is about *.93*), and it is not necessary to paint it in order to enhance IR radiation detection.

To study the appearance of Goertler vortices in both 2D and 3D hypersonic viscous interaction regimes, two different types of wedge models have been tested. For the first one the interaction is caused by a solid flap with an angle $\delta = 15°$, made of a crosslinked elastomer (Rhodorsil RTV 147), which is placed downstream of a stainless steel flat plate (Fig. 2). The flat plate length ($L = 126.9mm$) is such that the interaction is laminar for all the tested Reynolds numbers. The 3D interaction has been obtained by means of a *15°* RTV flap located downstream of a (stainless steel) delta wing having length and span equal to those of the flat plate. Also for RTV its relatively low thermal diffusivity coefficient ($\alpha = 2.34x10^{-7} m^2/s$) allows one to use the thin film sensor to correlate wall temperature to heat transfer coefficient.

The AGEMA Thermovision 880 IR camera, connected to the TIC 8000 A/D board has been employed to obtain the data hereafter presented. Details about the IR system and the *viewing* procedure may be found in Ref.[19]. In order to achieve a small field of view, i.e. the highest possible spatial resolution of the IR system (the expected vortices wavelength ranged from about 2 to 6mm), proper extension rings have been used in conjunction with the standard 7° IR lens.

For the concave wall models the surface temperature map has been recorded over small measurement frames (either *35x35mm*^{2} or *47x47mm*^{2}) located all on the symmetry axis and centered 82.5, 125.0, 170.0 mm from the leading edge, respectively. However, for the model b) only, being this last shorter than the other two, the frame centered at 170 mm has been moved upstream to 140mm.

To study the 2D viscous interaction caused by a wedge, a measurement frame of *35x35mm*^{2} has been used; such a frame is located on the flap, typically centered with respect to the longitudinal symmetry axis and with a side flush with the flap trailing edge. For the 3D interaction problem (delta wing/flap model) tests have been carried out with a measurement frame of *21x21mm*^{2}. In this last case, due to the three-dimensional characteristics of the reattaching flow, the frame has been located at different positions on the flap. For all the tests, to avoid the model span to be scanned along the vertical scanning direction of IR camera for which it has a spatial resolution lower than for the horizontal one, the camera itself has been kept 90° rotated around its roll axis. Calibration of IR system has been performed in the same *viewing* conditions taken during the tests.

The system software for the acquisition and preliminary handling of the (coloured) thermal image (a frame of *140x140* pixels composed of two interlaced fields) is the Computer Aided Thermography System (CATS). An application software has been also developed[19], which in particular yields the dimensionless heat transfer coefficient expressed in terms of Stanton number, basically is defined as

$$St = \dot{q}_c/[\rho \, c_p \, V \, (T_o - T_w)] \qquad (1)$$

where ρ, V, and c_p are respectively the mass density, the velocity and the specific heat at constant pressure of the free stream. As already mentioned, the history of the measured wall temperature T_w is related to the net wall heat flux $\dot{q}$ ($\dot{q} = \dot{q}_c - \dot{q}_r$, $\dot{q}_c$ and $\dot{q}_r$ being the convective and radiative heat fluxes, resp.) by using the thermal model of the thin-film sensor. For the concave wall models, in order to compare experimental and numerical data, it is convenient to use the standard definition of Stanton number based on the adiabatic wall temperature, T_{aw}, which is evaluated via the recovery factor r[20].

To quantitatively estimate the effect of the presence of Goertler vortices on the surface heat transfer distribution, it has been necessary to include into the data post-processing software an image restoration algorithm, that takes into account both electro-optical and lateral thermal conduction degradations. Thermogram restoration has been performed by means of a FFT inverse filter algorithm:

$$f(x,y) = \mathfrak{F}^{-1}\left\{G(\nu,\mu)/H(\nu,\mu)\right\} \qquad (2)$$

where $f(x,y)$ is the restored thermogram as a function of the spatial coordinates x and y, G is the Fourier Transform of the recorded (degraded) image, and H is referred to as the generalized *System Transfer Function*. Both G and H are functions of the spatial frequencies ν and μ. Imaging and sampling as well as lateral thermal conduction effects may be accounted for by means of the *Average Sampled System Modulation Transfer Function* (*ASSMTF*) and of the *Temperature Amplitude Transfer Function* (*TATF*), respectively [20]. By assuming cascaded the above effects, the relationship $H = ASSMTF \times TATF$ may be employed to solve eq. (2).

III.Results

III.1 Concave wall models

The relief surface temperature distribution presented in Fig. 3 is relative to a measurement frame recorded on the model b) and centered *125mm* from the leading edge. Testing conditions are: $M = 7.0$, $Re_m = .89x10^7/m$, zero angle of attack (the arrow indicates the stream direction). Data have been taken *1.12s* from the injection instant. The presence of the vortices produces the temperature periodic variation whose amplitude increases downstream (the average wavelength is about *8mm*). Testing conditions correspond to a spatial frequency for which a limited data correction is needed to account for imaging and sampling as well as lateral conduction degradations. The plot of Fig.

3, however, does not have such corrections, but only a weak smoothing on the recorded data.

Since neither mean velocity or turbulence measurements have been done in the present investigation, one has tried to verify that the wall temperature fluctuations are caused by Goertler vortices by checking the following two points: 1) the flow upstream of the (presumed) vortices onset is laminar; 2) the heat transfer fluctuations are not due to turbulence induced by the model roughness.

To do this, it has been convenient to evaluate the Stanton longitudinal distribution, averaged along the spanwise direction, and to compare it with a theoretical solution of laminar hypersonic boundary layer over flat plate[21]. For a typical testing condition ($M = 7.0$, $Re_m = 1.22x10^7/m$, model c), Fig. 4 depicts this comparison where the experimental dashed curve has been obtained by matching data taken over three measurement frames located on the symmetry axis at differents streamwise locations. The comparison seems to be good within a reasonable accuracy level all along the model flat part and confirms the boundary layer laminar development there. Starting from the beginning of the curved part of the model (in the present case, $x = 100mm$), as expected the measured values of Stanton number begin to rise because of the decrease of Mach number due, in turn, to the compression waves effect.

The problem of determining what induces the subsequent (at $x \simeq 150mm$) steep rise of heat transfer and its fluctuations is harder. From data reported in Ref.[22] it appears that the transition length should be greater than the flat plate length of the present models, but it is known that one must be very cautious in using this kind of data, because they strongly depend on the wind tunnel and model conditions.

Anyhow, the quite regular structure of the heat transfer fluctuations observed in practically all the testing conditions seems to exclude that such fluctuations may be caused by turbulence induced by surface roughness . It is rather more likely that Goertler vortices develop in the (initially laminar) unstable boundary layer: Goertler disturbances together with Tollmien-Schlichting waves could give rise to a (premature) onset of turbulence, which seems to be confirmed by the circumstance that the Stanton number values over the curved wall rise to the typical order of turbulent regime. Additional tests are strongly recommended in order to determine to an higher reliability level the transition Reynolds number for present testing conditions.

Note that the presence of Goertler vortices in hypersonic flow concave wall models (weak compression ramps) induces heat transfer fluctuations (data are not reported in this paper) whose amplitude (relative to the mean value) is generally lower than that measured in the reattaching flow zone in a typical boundary layer/shock wave interaction caused by a wedge.

The measured wavelength values, λ have been reduced so as to obtain the pairs of experimental values (G, γ) reported in Fig. 5 (open symbols) where they are superimposed to the stability diagram of Ref[10], which is relative to the same flow conditions of present tests, i.e. $M = 7$ and $T_w/T_{aw} = 0.5$. The wavenumber has been evaluated as $\gamma = 2\pi L/\lambda$. The characteristic length L, appearing also in the definition of Goertler number

$$G = Re_m \, L(L/\Re)^{1/2} \qquad (3)$$

has been taken to be proportional to the conventional boundary layer thickness, $L = x/(Re_x)^{1/2}$, where Re_x is the local Reynolds number based on the distance x from the leading edge, and x represents the streamwise location where vortices seem to be well developed.

As is evident, experimental points are all located in the region where the disturbances have to be amplified according to the linear theory. On the other hand, the theory cannot predict anything about the wavenumber that will actually appear for given experimental conditions because any external factor imposed on the flow may affect the activation of the instability mechanism. Hence, depending on the particular experimental apparatus (e.g. nozzle, wind tunnel screens, model surface), the disturbances corresponding to a certain wavelength are only excited. For this reason, the average value of Goertler number based on the vortices wavelength, Λ, obtained for present measurements ($\Lambda \cong 3500$) does not agree with the theoretical value ($\Lambda \cong 1800$) corresponding to the maximum total amplification. Both experimental (continuous line fitting the data points) and numerical (dashed line) loci $\Lambda = const$, which in the plane $G - \gamma$ are straights whose slope is equal to 3/2, are drawn in Fig. 5. Note also that, according to previous experimental findings (referring to subsonic flow), present Λ experimental value is greater than that predicted numerically.

III.2 Wedge models

Thermogram of Fig. 6 shows a typical restored surface temperature map (relative to a $35x35mm^2$ frame) recorded on the flap downstream of the flat plate model. Testing conditions are: $M = 7$, $Re_m = 1.4x10^7/m$, zero angle of attack. Time at which the picture has been taken during the test run from the injection instant is $t = 1.12s$. The flow comes from the bottom of the thermogram and the horizontal periodic variation of the temperature is to be correlated to the presence of the spanwise vortices. The average measured wavelength is about 3.7mm. The AGEMA 880 system, with the 7° lens coupled with 12+20mm extension rings, used at the minimum focus distance, in these conditions works at a spatial frequency for which a limited data correction is needed to account for imaging and sampling, as well as lateral conduction degradations. The entity of these corrections is detailed by the plot of Fig. 7 where the Stanton number spanwise profile along the black line drawn on the thermogram of Fig. 6, is shown. In Fig. 7 the dashed line represents the coarse data, the dotted line the ones restored from imaging and sampling degradation effects, the continuous line the final result which takes into account also the lateral conduction degradation. As may be seen, corrections are generally restricted within 10%. The average level of Stanton number as measured in the present test well agrees with that reported by other authors[11,12]. The two biggest St peaks cleary evident in Fig. 7, and the related almost white two slender regions located at the lateral edges of the thermogram, are probably due to some irregularities of the free stream caused by the nozzle.

Table I summarizes the averaged wavelength value, λ, measured on the two tested wedge models, for various Mach and Reynolds numbers. For the delta wing/flap configuration the measurement frame is located on the flap with its center *20mm* from the hinge line and *20mm* from the side edge. As a general trend the vortices wavelength is smaller for the 3D interaction than for the 2D one; in all the cases it decreases as Reynolds number increases. Mach number seems to have a minor influence, at least within the limited range of values of present tests.

As already seen, the (2D) linear theory of Goertler instability predicts that the Goertler number based on the vortices wavelength, Λ, must be constant. The relation $\Lambda = const$ qualitatively agrees with the experimental trend that the wavelength decreases as Reynolds number increases. However, it should be noted that for present results the product $Re_m \lambda^{3/2}$ slightly decreases as the unit Reynolds increases. On the basis of the linear theory it may be concluded that there is a corresponding decreases of the (mean) curvature radius of the dividing streamline. Indeed, the separation region extent reduces as Re_m increases and the corresponding reduction of the (mean) curvature radius is confirmed.

The nature of 3D interaction is more complex. Recently present authors carried out some experimental tests to visualize the surface flow field over the delta wing/flap configuration as well as to measure the related average wall heat transfer distribution[16]. Measurements, made by means of a computerized IR imaging system, revealed that a mixed-type separation occurs over the delta wing, with a transitional (or turbulent) regime near the centerline and a laminar flow at the lateral edges of the delta wing. In the latter case, in fact, the local Reynolds number is lower due to the shorter distance from the leading edge. The streamwise Stanton number distributions recorded on the delta wing symmetry axis ($y/S = 0$) and along the line $y/S = 0.24$ (S being the flap span) are shown in Fig. 8, for $M = 8.15$ and $Re_m = 1.26x10^7/m$. These two trends uncover the two different turbulent and laminar, respectively, flow behaviors as discussed in Ref.[11] for a two-dimensional flow.

Of course, one has to be very cautious in extending 2D flow characteristics to 3D situations because in this last case the presence of a crossflow makes the boundary layer unstable (i.e. transition Reynolds numbers are typically lower than the corresponding 2D values) and can

FLAT PLATE				DELTA WING			
$M = 7$		$M = 8.15$		$M = 7$		$M = 8.15$	
$Re_m \times 10^{-7}$	λ (mm)	$Re_m \times 10^{-7}$	λ (mm)	$Re_m \times 10^{-7}$	λ (mm)	$Re_m \times 10^{-7}$	λ (mm)
.95	6.0	1.2	6.2	.95	3.1	1.3	2.5
1.1	4.8	1.8	3.9	1.5	2.1	1.9	2.2
1.4	3.7			2.1	2.0		
1.5	3.6						

Table I

invalidate the assumption of local 2D flow along each longitudinal direction. Anyhow,a shorter vortices wavelength is to be expected on the flap centerline than in the lateral zones. In fact, oil film flow visualizations show(13) that the turbulent separation line is remarkably moved downstream, practically coinciding with the hinge line at the highest Reynolds numbers. Thus, the streamline curvature radius is relatively smaller. In effect, the thermograms (not shown herein) relative to 3D interactions do not show apparently the presence of vortices on the flap symmetry axis . This is most probably due to the limited spatial resolution of IR system which does not allow to resolve extremely small wavelengths. Even though over the lateral regions the nature of the 3D interaction is laminar, a higher turbulence level than the corresponding 2D case is to be expected there, due to the presence of the crossflow that produce a premature onset of turbulence. Therefore, the vortices wavelength on the flap lateral zones in 3D flow seems to be shorter than in 2D flow.

IV.Conclusions

An experimental investigation has been carried out to analyse the development of Goertler vortices due to an unstable hypersonic boundary layer and their effects on the wall heat transfer. Measurements, made by means of a computerized IR imaging system, have been performed in a wind tunnel at Mach number equal to 7 and *8.15* for different Reynolds numbers. Tested models, consisting of concave walls placed downstream a flat plate, as well as of 2D and 3D wedge configurations, are made of NORCOAT or RTV, low thermal conductivity material used to better visualize the heat transfer fluctuations by means of the *IR* thermographic technique.

The presence of Goertler vortices has been successfully detected through the spanwise periodic variation of the wall heat transfer coefficient. Due to the limited spatial resolution of the IR system, a proper data correction (image restoration) has been needed, which takes into account the degradation effects due to both the IR system and the lateral thermal conduction. It has been found that the fluctuations of the wall heat transfer coefficient are higher over the wedge models for which they range from 20 to 30% with respect to the spanwise average value.

The (non-dimensional averaged) vortices wavelength measured over the concave models has been correlated to the Goertler number based on the vortices wavelength and compared to a numerical stability diagram of the literature. Data fall all into the instability region and the slope of the correlation straight agrees with that theoretically predicted. However, the value of Λ found in the present tests is higher than the numerical one because the physical selection mechanism of the disturbances strongly depends on the particular experimental apparatus (that is not modeled by the numerical code). This finding is consistent with other previous experimental observations.

As regards the wedge models, it has been found that the vortices wavelength is smaller for 3D interaction than for 2D interaction; in both cases it decreases as unit Reynolds number increases. Mach number seems to have a minor influence, at least within the limited range of tested values. For these models, the experimental findings have been found to agree with theoretical predictions based on the interaction nature and on the linear theory of the Goertler instability.

V.Acknowledgments

Present work has been supported by grants of CIRA (Centro Italiano Ricerche Aerospaziali) and Avions Marcel Dassault.

Authors are indebted to prof. T. Alziary de Roquefort and dr. D. Aymer de la Chevalerie because tests were carried out at CEAT wind tunnel (Poitiers) on models made at CEAT.

References

(1) Winoto S.H. and Low H.T., Transition of Boundary Layer Flows in the Presence of Goertler Vortices, Exp. Fluids, 10, 281-284 (1991)

(2) Kottke V. and Mpourdis B., On the Existence of Taylor-Goertler Vortices on Concave Walls, in Flow Visualization IV (ed. Véret C.), 475-480, Hemisphere (1987)

(3) Floryan J.M. and Saric W.S., Stability of Goertler Vortices in Boundary Layers, AIAA J., 20, 316-324 (1983)

(4) Liepmann H.W., Investigation of Boundary Layer Transition on Concave Walls, NACA Wartime Report, ACR 4J28 (1945)

(5) Bippes H., Experimental Study of the Laminar-Turbulent Transition on a Concave Wall in a Parallel Flow, NASA TM-75243 (1978)

(6) Ginoux M., Streamwise Vortices in Reattaching High-Speed Flows: a Suggested Approach, AIAA J., 9, 759-760 (1971)

(7) El-Hady N.M. and Verma A.K., Growth of Goertler Vortices in Compressible Boundary Layers Along Curved Surfaces, J. Eng. Appl. Sc., 2, 213-238 (1983)

(8) Spall R.E. and Malik M.R., Goertler Vortices in Supersonic and Hypersonic Boundary Layers, Phys. Fluids A, 1, 1822-1835 (1989)

(9) Jallade S., Etude theorique et numerique de l'instabilité de Goertler, PhD thesis, Polyt. of Toulouse (1990)

(10) Aymer de la Chevalerie D., Creff J.L. and Fontaneau J.L., Tourbillons de Taylor-Goertler, CEAT Rept., Poitiers (1991)

(11) Delery J. and Coet M.C., Shock-shock and Shock Wave/Boundary Layer Interactions in Hypersonic Flows, AGARD VKI Special Course on Aerothermodynamics of Hypersonic Vehicles (1988)

(12) Simeodines G. and Wendt J., Shock Wave Boundary Layer Interactions in Compression Corners at Mach 14, Hermes Wind Tunnel Meeting, Capua (1990)

(13) Alziary de Roquefort T., Interaction onde de choc-couche limite en ecoulement hypersonique tridimensional transitionnel, CEAT Rept (1987)

(14) de Luca L. and Cardone G., Experimental Analysis of Goertler Vortices in Hypersonic Wedge Flow, Thermosense XIV SPIE meeting, Orlando 1992

(15) Inger G.R., On the Curvature of Compressible Boundary Layer Flows Near Separation, J. Appl. Math. & Phys., 28, 1027-1035 (1977)

(16) de Luca L., Cardone G., Carlomagno G.M., Alziary de Roquefort T. and Aymer de la Chevalerie D., Infrared Measurements of Aerodynamic Heating in Hypersonic Wind Tunnel, in Aerothermodynamics for Space Vehicles, Battrick B. ed., ESA SP-318, 229-234, (1991)

(17) Alziary de Roquefort T., Les souffleries hypersoniques du centre d'etudes aerodynamiques et thermiques de Poitiers, 22eme colloque d'aerodynamique appliqueé, Lille (1985)

(18) de Luca L., Computerized IR Thermography for Convective Heat Transfer Measurements, in Computational Methods and Experimental Measurements V, (eds. Sousa A., Brebbia C.A. and Carlomagno G.M.), 347-358, CMP/Elsevier (1991)

(19) de Luca L., Cardone G., Carlomagno G.M., Aymer de la Chevalerie D. and Alziary de Roquefort T., Flow Visualization and Heat Transfer Measurements in Hypersonic Wind Tunnel, Experimental Heat Transfer, 5, 65-79, (1992)

(20) de Luca L., Cardone G and Aymer de la Chevalerie D., Goertler Instability of Hypersonic Boundary Layer, submitted to Exp. Fluids (1992)

(21) Shapiro A.H., The Dynamics and Thermodynamics of Compressible Fluid Flow, The Ronald Press Company, New York (1954)

(22) Srinivasan P., Etude des effects d'interaction et de decollement tridimensionnel de la couche limite en regime laminaire supersonique, PhD thesis, Poitiers (1973)

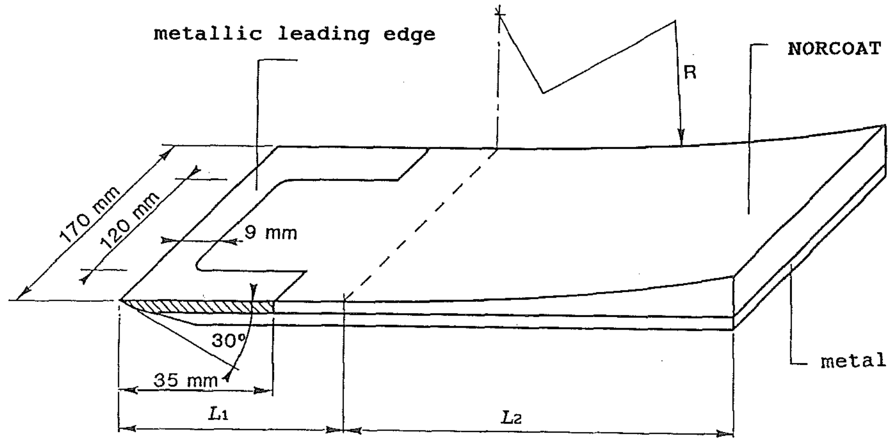

Fig. 1 Concave wall model (courtesy of CEAT, Poitiers)

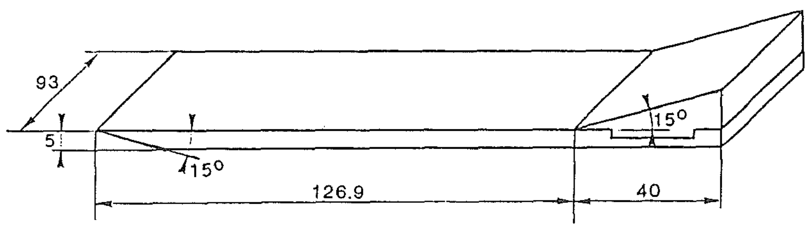

Fig. 2 Flat plate/wedge model (courtesy of CEAT, Poitiers)

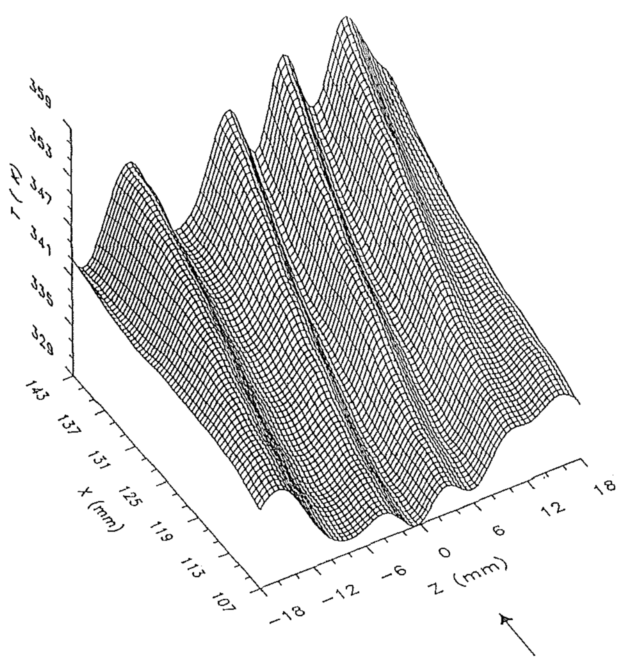

Fig. 3 Relief surface temperature map taken on the concave wall model b)

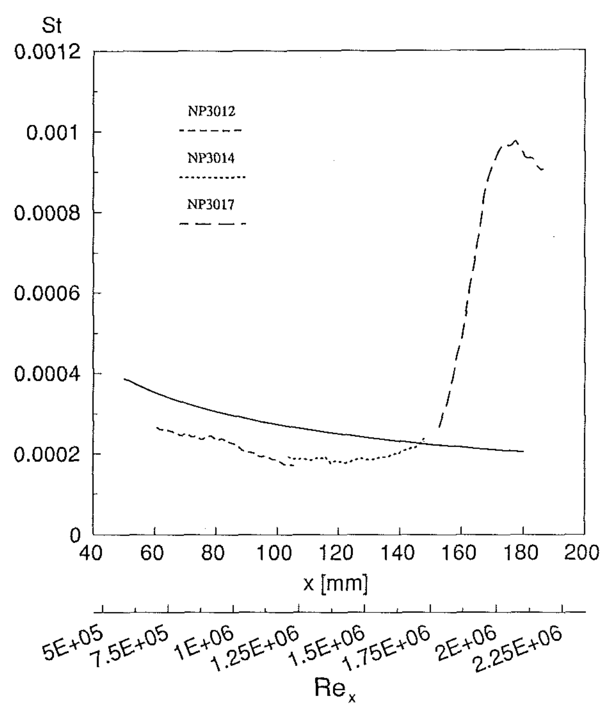

Fig. 4 Comparison between measured and computed longitudinal *St* distributions over model c)

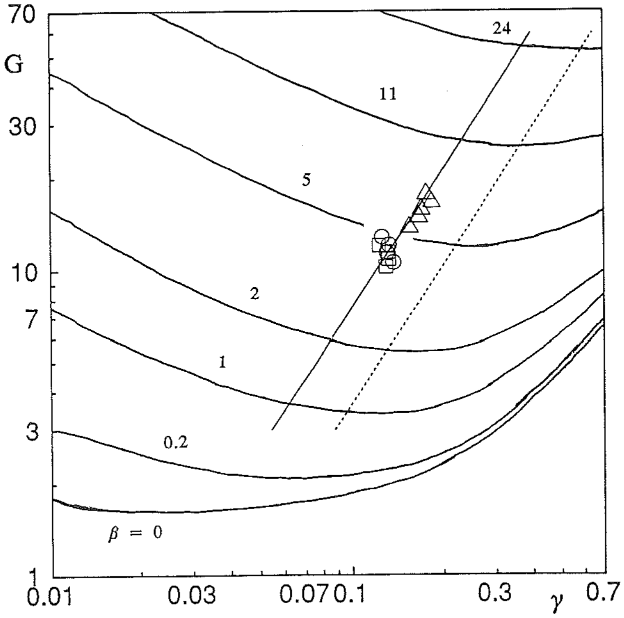

Fig. 5 Correlation of present experimental data as compared to the numerical one of Ref.(10)

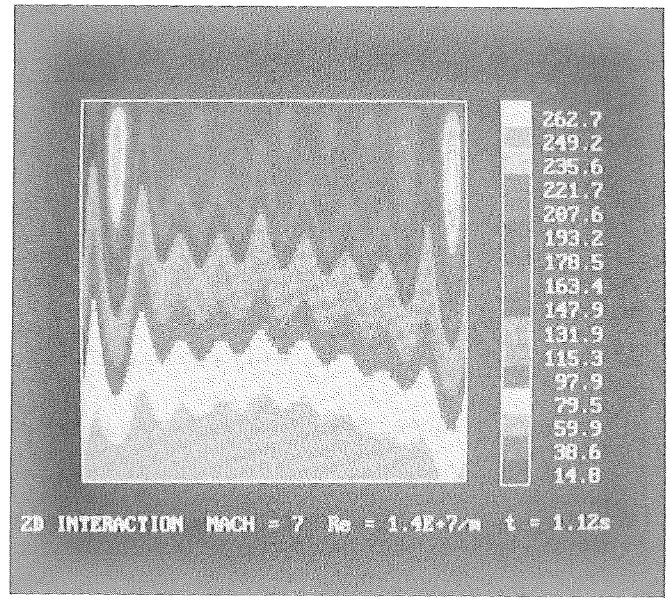

Fig. 6 Restored surface temperature map over the 2D wedge model

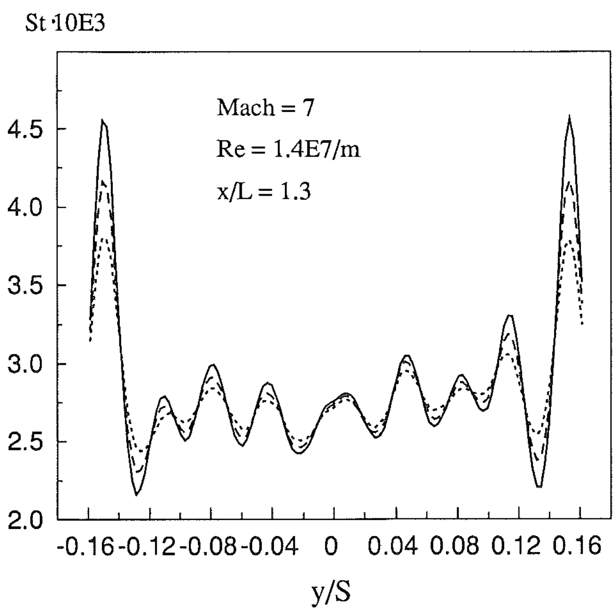

Fig. 7 Stanton number spanwise distribution

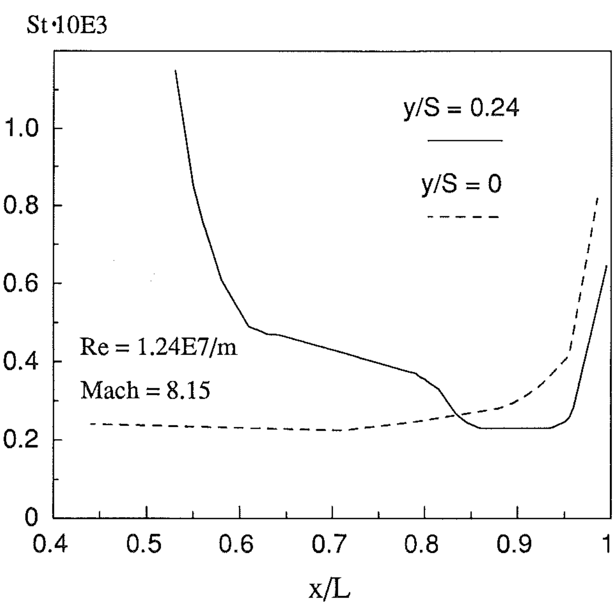

Fig. 8 Stanton number streamwise distributions over the delta wing model